Journal of Engineering Science and Technology
Vol. 12, No. 8 (2017) 2046 - 2063

OPTIMIZATION STUDIES FOR THE FLOTATION OF BUNKER OIL FROM CONTAMINATED SAND USING MICROBUBBLES

M. W. LIM, E. V. LAU*, P. E. POH

School of Engineering, Monash University Malaysia, Jalan Lagoon Selatan,
47500 Bandar Sunway, Selangor Darul Ehsan, Malaysia
*Corresponding Author: lau.ee.von@monash.edu

Abstract

This paper studies the optimization of microbubble-aided (Sauter diameter: 80 μm) flotation technology to separate high density bunker oil from oil-wet sand using response surface methodology (RSM). A second order response function was used to model the flotation efficiency under the influence of pH, temperature, experimental duration and input flow of microbubbles. The optimum flotation parameters were found to be at temperature of 60 ^{o}C, pH 8, duration of 20 minutes, and input flow of 6L/min with a predicted maximum flotation efficiency of 40.4%. This was in good agreement with the flotation experimental results of 40.1%. In comparison with the control study, the natural flotation efficiency of bunker oil was only 2.9% which reinforces the fact that the presence of microbubbles could aid the removal of oil from sand. Nevertheless, the oil-wet conditions prove difficult for efficient removal of oil contaminant. The oil contaminant was easily removed in water-wet conditions, whereby increase in water content from 0 wt% to 8 wt% increased the removal efficiency from 40.1% to 76.2% under same optimum flotation conditions. This was attributed to the presence of thin film of water which weakens the attractive force between sand and oil layer.

Keywords: Oil spills; Flotation technology; Microbubbles; Bunker oil; Response surface methodology; Oil-wet.

1. Introduction

Marine oil spills are known to cause devastating impacts on environment, economy and society. The long-term impact of oil spills highlights the necessity and urgent need for a quick and efficient method for removal of oil contamination. Flotation technology is a promising remediation method which is adopted for the removal and recovery of oil from contaminated sand/soil due to its

Nomenclatures

a_i	Surface area of air bubble
D_{32}	Sauter mean diameter
D_{ave}	Average diameter of air bubbles
D_c	Diameter of flotation column
D_i	Diameter of air bubble
e	Random error
k	Number of studied factors
$\dot{N}$	Air bubble flux
n	Number of air bubbles
Q	Gas volumetric flow rate
S_b	Specific Surface Area
v_i	Volume of air bubble
X_1	Input variable [Effect of temperature (^{o}C)]
X_2	Input variable [Effect of pH]
X_3	Input variable [Effect of experimental duration (min)]
X_4	Input variable [Effect of input flowrate (mL/s)]
X_i	Input variables
X_j	Input variables
Y	Output variable (Flotation efficiency)

Greek Symbols

β_0	Constant coefficient
β_i	Interaction coefficients of linear terms
β_{ii}	Interaction coefficients of quadratic terms
β_{ij}	Interaction coefficients of second-order terms

Abbreviations

3-D	Three dimensional
ANOVA	Analysis of Variance
CST	Centistokes
CCD	Charged Coupled Device
DOE	Design of Experiments
FO	Fuel oil
ID	Inner diameter
OD	Outer diameter
RSM	Response Surface Methodology

ability for separating very small or light weight particles with low settling velocities. This technology utilises the difference in surface properties of both contaminant and soil. The mechanism of flotation lies in the generation of gas bubbles that attach themselves by colliding with the hydrophobic contaminant, forming a bubble-particle attachment. The bubble-particle attachment is buoyant, therefore it rises to the surface of the liquid, creating a layer of separated particles which could be recovered (Fig. 1) [1].

Hence, the presence of air bubbles is advantageous for flotation purposes. The attachment of bubbles onto the oil contaminant increases the bubble-particle buoyancy which would therefore increase the floatability of the contaminant in a

liquid medium. While there are many investigations that reported on the usage of microbubbles flotation of oil from contaminated soil [2-7], the optimization of these processes has not been significantly investigated. In the event of an oil spill on beach sands, an optimum operating condition is essential not only to maximize the oil removal but also to reduce operating costs.

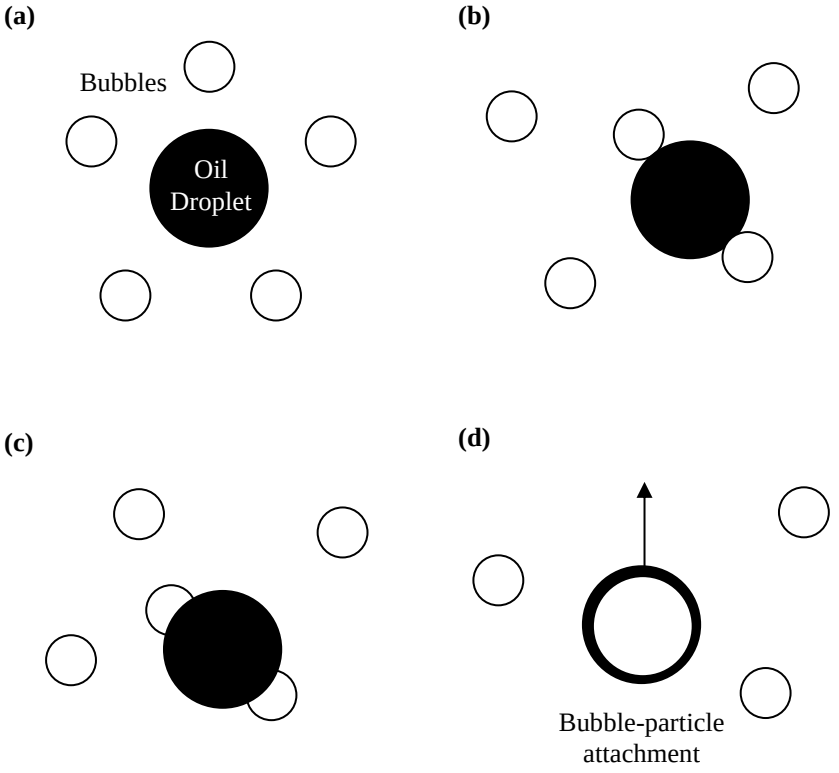

Fig. 1. Mechanism of flotation: (a) generation of gas bubbles for flotation of oil contaminant, (b) bubble collision onto oil contaminant, (c) bubble attachment with oil contaminant, (d) formation of stable bubble-particle attachment followed by subsequent flotation [1].

There are many operating parameters that could affect the flotation efficiency, which is broadly classified into chemical parameters (pH [6, 8] and surfactant addition [9, 10]), physical parameters (temperature [10-12], aging period [5, 13], wettability [14-16]) and hydrodynamics parameters (bubble characteristics [1, 17]). To determine the optimum flotation parameters, many sets of flotation experiment have to be conducted due to the vast factors involved. This may not be feasible, as it would consume a lot of time and resources due to the number of sets involved. In addition, these experiments are also incapable of reaching the true optimum as they do not explore the possibility of interactions among parameters [18].

The response surface methodology (RSM) is adopted in this study as an efficient modelling method to simplify the determination of optimum flotation parameters. RSM is a statistical and mathematical technique as well as an

efficient method used for development, improvement, and also to obtain the optimized parameters required based on desirability [19, 20]. The design of experiments (DOE) could study the effect of independent parameters and their responses using minimum number of experiments, therefore effectively reducing the number of experimental sets required to evaluate the different parameters [21]. This method also helps to observe and understand the interaction effects between the controllable parameters.

The aim of this work is to evaluate and optimize the removal of oil from contaminated sand via flotation technology using microbubbles. In this study, the flotation process was attempted on dry sands contaminated with oil (oil-wet sands) for the removal of bunker oil. The contaminant is considered difficult to be removed in an oil-wet sand condition due to the high attachment forces between the oil and sand particles. Hence, the influence of physical and chemical parameters could be easily observed through a significant change in the flotation efficiency. The effects of temperature, pH, input water flow rate and experimental period were studied and optimized using RSM to achieve the maximum flotation efficiency in this study. The main effect of these parameters and their interactions were also studied on their effect on flotation performance. Finally, the optimized flotation parameters were used to study the effect of wettability in the contaminated oil sand.

2. Materials & Methodology

2.1. Materials

High density bunker oil was obtained from KIC Oil Terminals in Port Klang, Malaysia. The type of oil used was fuel oil with a maximum viscosity of 380 Centistokes (FO 380 CST). Sand samples were obtained from a clean designated site from the shores of Port Klang, Malaysia. Analytical grade sodium hydroxide solution (NaOH, Sigma-Aldrich, Malaysia) was used to adjust the slurry pH.

2.2. Methodology

2.2.1. Preparation of oil-wet contaminated sample

Sand was initially air-dried overnight to remove moisture content. Dry sieving was then carried out to remove the debris (leaves, wood, stones and gravel) and to separate the sand into its respective particle sizes (1000 μm, 500 μm, 250 μm, 125 μm) using a Retsch AS 200 sieve shaker. An oil-wet sand condition were prepared by mixing a known mass of bunker oil (200 g) into a 5 L beaker containing 500 g of dry sand sample with particle size ratio as summarized in Table 1. The mixture is allowed to mix homogeneously overnight before flotation experiments.

Table 1. Ratio of sand content with respect to particle size.

Particle Sizes (μm)	Particle Size Range (μm)	Percentage (%)
1000	1000-2000	60.0
500	500-1000	20.0
250	250-500	10.0
125	125-250	10.0

2.2.2. Microbubble generation

The microbubbles were generated via venturi (tubule diameter: 0.5cm; inlet and outlet diameter: 1.5 cm) through hydrodynamic cavitation. The microbubbles generated were characterized using a Charge Coupled Device (CCD) camera. The equipment used for the imaging process were Precision borescope (Hawkeye, US Patent 5361166), CCD Camera (QImaging Retiga 200R), and 200W light source (Dolan-Jenner Fibre-Lite MH-100). The images were analyzed by utilizing image processing software (QCapture Pro). A total of 150 images were captured at 1 frame per 10 miliseconds for each analysis, and a total of 500 bubbles were analyzed.

The bubbles were characterized based on the average and Sauter bubble diameter, specific surface area and air bubble flux. The average bubble diameter, D_{ave} is defined as sum of air bubble diameters, D_i over the total number of air bubbles, n as shown in Eq. (1).

$$D_{ave} = \frac{\sum D_i}{\sum n} \tag{1}$$

On the other hand, the Sauter mean diameter, D_{32} is defined as the sum of equivalent spherical diameter, D_i over the number of air bubbles, n as shown in Eq. (2). D_{32} represents the average bubble diameter with the same total bubble volume to surface area ratio as the mean bubble size distribution. Sauter mean diameter is a more accurate representation of the average bubble diameter in a bubble distribution [22]. Therefore, the Sauter mean diameter values would be adopted in the subsequent sections of this report, unless otherwise stated.

$$D_{32} = \frac{\sum n.D_i^3}{\sum n.D_i^2} \tag{2}$$

The specific surface area of air bubbles is defined as the ratio of surface area, a_i to volume of bubbles, v_i in Eq. (3). This property is especially important in oil flotation as the attachment of bubbles to oil occurs on the surface. A higher specific surface area translates into higher probability of oil attachment to bubble surface which would therefore lead to increased oil recovery.

$$S_b = \frac{\sum {}^{a_i}/_{v_i}}{n} \tag{3}$$

Lastly, the air bubble flux, $\dot{N}$ is defined as the amount of air volumetric flow rate, Q per cross sectional area of flotation column and average bubble volume per Eq. (4).

$$\dot{N} = \frac{Gas\ volumetric\ flowrate, Q}{(Cross\ sectional\ area\ of\ flotation\ column)(Average\ bubble\ volume)}$$
$$= \frac{Q}{\left(\frac{\pi {D_C}^2}{4}\right)\left(\frac{\pi {D_{32}}^3}{6}\right)} = \frac{24Q}{(\pi D_C)^2 (D_{32})^3} \tag{4}$$

2.2.3. Microbubble flotation experiments

To evaluate the effect of microbubbles on bunker oil flotation, the flotation experiments were carried out in a laboratory-scale flotation cell (7" diameter, 10.5" height) via a closed loop system as shown in Fig. 2. The water flow rate entering the venturi ranges from 2-6 L/min, and was adjusted through a ball valve and flow meter. A centrifugal pump is used to circulate water for the generation of microbubbles. The

desired microbubbles were produced due to the difference in pressure at the venturi throat (ID & OD: 8mm, throat diameter: 3mm).

The RSM studies were carried out to optimize the microbubble-assisted flotation, and the parameters chosen for this study are temperature, pH, duration of experiment and input water flow rate. The optimum parameters will be determined based on the model obtained through RSM.

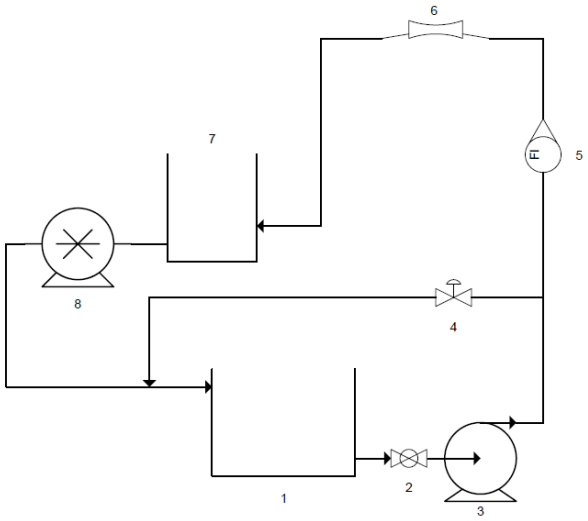

Fig. 2. Schematic diagram of flotation experiment setup using microbubbles [1-Water source, 2-Ball valve, 3-Centrifugal pump, 4-Diaphragm valve, 5-Rotameter, 6-Venturi, 7-Flotation cell, 8-Peristaltic pump].

2.2.4. Response surface methodology (RSM)

The design of experiments (DOE) were carried out using the Design Expert 6.0.8. A central composite design (CCD) model was chosen to fit the second-order models, as it contains an embedded factorial design with center points that is augmented with a group of axial points that allow estimation of curvature. It consists of a 2^k factorial with *nF* factorial runs (points with all possible combination of minimum and maximum values of control parameters), 2*k* star runs (minimum/maximum value, with other parameters being nominal values), and *n*C center runs (control parameters set at nominal value).

A total of 30 runs were conducted to observe the effect of experimental parameters. Six runs were repeated at the design center to evaluate the pure error of the equation. Eq. (5) shows the quadratic model used to estimate the optimal point:

$$Y = \beta_0 + \sum_{i=1}^{k} \beta_i X_i + \sum_{i=1}^{k} \beta_{ii} X_i^{\,2} + \sum_{i_{i\leq j}}^{k} \sum_{j}^{k} \beta_{ij} X_i X_j + \ldots + e \quad (5)$$

where Y is the output, X_i and X_j are input parameters, β_0 is constant coefficient, β_i, β_{ii} , β_{ij} are interaction coefficients of linear, quadratic and second-order terms respectively, k is the number of studied parameters, and e is the random error. A second order model was used to fit the response, while the coefficients of the model was then calculated using a multi-linear regression analysis. The interactive effects

between the four parameters are then plotted in 2D and 3D contour plots. The optimum parameters are determined based on the model obtained through RSM.

3. Results and Discussion

3.1. Microbubbles characterizations

Table 2 shows a comparison of the air bubble parameters with respect to water flow rate through the venturi, water temperature and pH. It should be noted that the experiments were carried out at room temperature, natural distilled water pH and input flow rate of 3L/min unless otherwise stated.

Table 2. Summary of microbubble characterizations.

	Flow rate (L/min)				
	2	**3**	**4**	**5**	**6**
Average diameter, D_{ave}(µm)	189.11 [42.79]	177.24 [23.22]	168.65 [27.03]	159.22 [28.19]	151.60 [26.94]
Sauter mean diameter, D_{32} (µm)	144.85	92.92	89.91	86.19	81.89
Specific Surface Area, S_b (x 10^5) (m^2/m^3)	0.78	0.83	1.02	1.25	1.47
Air bubble flux, $\dot{N}$ (x 10^6) ($1/m^2.s$)	0.50	2.41	2.93	3.83	5.06
	Temperature (^oC)				
	20	**30**	**40**	**50**	**60**
Average diameter, D_{ave}(µm)	169.83 [38.57]	165.07 [35.02]	168.65 [37.85]	171.83 [38.25]	164.44 [35.48]
Sauter mean diameter, D_{32} (µm)	119.59	107.85	114.02	114.88	107.44
Specific Surface Area, S_b (x 10^5) (m^2/m^3)	1.08	1.18	1.15	1.10	1.21
Air bubble flux, $\dot{N}$ (x 10^6) ($1/m^2.s$)	1.24	1.70	1.43	1.40	1.71
	pH				
	6	**8**	**10**	**12**	**14**
Average diameter, D_{ave}(µm)	168.65 [27.03]	158.35 [29.55]	155.07 [28.03]	150.26 [25.91]	149.58 [22.56]
Sauter mean diameter, D_{32} (µm)	89.91	91.64	84.46	80.27	70.47
Specific Surface Area, S_b (x 10^5) (m^2/m^3)	1.02	1.27	1.38	1.47	1.50
Air bubble flux, $\dot{N}$ (x 10^6) ($1/m^2.s$)	2.93	2.76	3.53	4.11	6.08

[a] Values are average of triplicates while values in bracket [] represents the standard deviation of bubble distribution

It can be observed from Table 2 that the increase in water temperature does not appear to affect the average bubble diameter and Sauter mean diameter for microbubbles. The average Sauter mean diameters across the five temperature points (20 - 60 ^{o}C) is approximately 112 μm with a small standard deviation of 7 μm. The lack of trend and low standard deviation between data across different temperatures indicate that the increase in fluid temperatures does not affect the bubble size or coalescence [23]. A two tail inequality t-Test was also conducted to test the null hypothesis that the temperature does not influence the bubble size diameters. At a 95% confidence level, the t-values fall outside the critical areas, and therefore the null hypothesis is not rejected. Hence, the observed difference between the bubble diameter is not significant with the increase in temperature, which signifies that the temperature of the liquid medium does not affect the bubble diameter generated.

Inversely, the increase in pH demonstrated a decreasing trend for microbubbles diameter size. This is attributed to the increase in sodium hydroxide adsorption at the gas-liquid (bubble-water) interface, which helps to stabilize the liquid film surrounding the bubble. This would therefore lead to a lower probability of bubble coalescence, hence the smaller bubble size [24]. Smaller bubble diameters results in an increase in air bubble flux and specific surface area of air bubbles as shown in Eqs. (3) and (4).

In Table 2, the results also showed that the increase in flow rate through the venturi lowers the average microbubble diameter and Sauter mean microbubble diameter generated. The increase in water flow rate decreases the static pressure at the tubule (throat) section. Due to the lower pressure with increasing flow rate, the air from atmosphere enters the venturi at a higher rate which leads to the increase in the mixing rate of gas and liquid which therefore decreases the bubble diameter generated.

3.2. Microbubble flotation experiments

The independent parameters used in this experimental study for the microbubble flotation method are temperature (^{o}C), pH, duration of flotation (mins) and water flow rate (L/min) entering the flotation cell, which are denoted as X_1, X_2, X_3 and X_4 respectively. The predicted response, flotation efficiency (%) is designated as Y. The independent parameters and their coded/actual values used in this study are shown in Table 3.

Table 3. Actual and coded values of independent parameters chosen for CCD design.

Parameter	Symbol	Code parameter level		
		Low -1	Center 0	High +1
		Actual value		
Temperature (^{o}C)	X_1	30	40	50
pH	X_2	8	10	12
Duration (min)	X_3	10	15	20
Flow rate (mL/s)	X_4	3	4	5

3.3. Regression model equation and analysis of variance (ANOVA)

In this experiment, a total of 30 CCD batch runs were conducted as shown in Table 4. The experimental results in Table 4 were fitted to a highest order polynomials model, with significant additional terms. The full quadratic second order model equation was not aliased and was therefore selected. Hence, the model equation representing the flotation efficiency using microbubbles (Y) was expressed as functions of temperature (X_1), pH (X_2), duration (X_3), and flow rate (X_4), for code unit as shown in Eq. (6) as below.

$$Y = 21.13 + 1.59X_1 + 2.01X_2 + 2.39X_3 + 2.07X_4 + 0.55{X_1}^2 + 0.55{X_2}^2 + 0.99{X_3}^2 + 0.73{X_4}^2 - 0.28X_1X_2 - 0.41X_1X_3 + 0.41X_1X_4 + 1.57X_2X_3 - 1.49X_2X_4 + 1.07X_3X_4 \quad (6)$$

A model adequacy check is important to ensure that the model used fits the experimental results, as misleading results could occur due to inadequate fit. Figure 3 shows the normal probability residual plot which was used for approximating the model. The figure showed that no response transformation is required to convert the data using any mathematical functions. Figure 4 on the other hand shows the studentized residual plot with respect to the predicted oil flotation efficiency. The studentized residual plot measures the standard deviation between the actual and predicted oil flotation efficiency value. A random scatter of data was observed in Fig. 4, which suggests a constant variance for all values of the response.

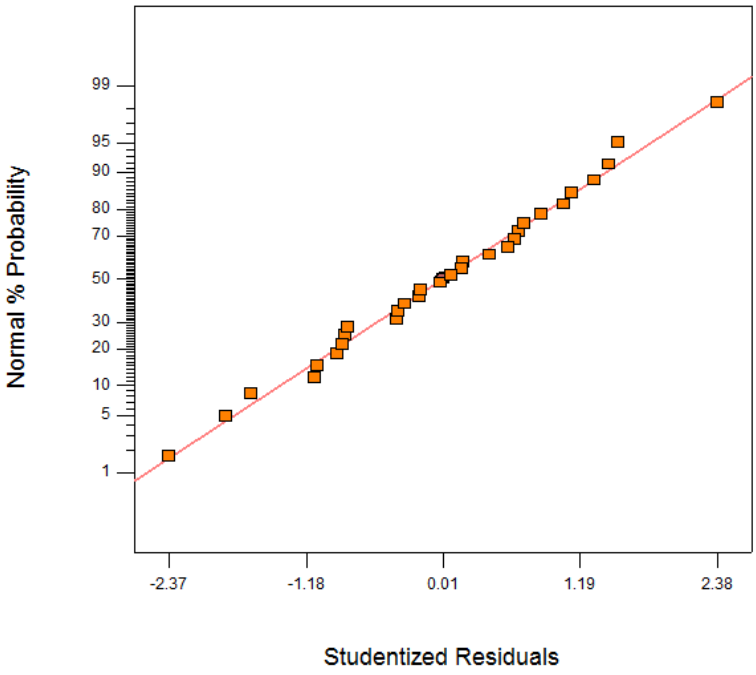

Fig. 3. Studentized residuals and normal percentage probability plot for oil flotation efficiency.

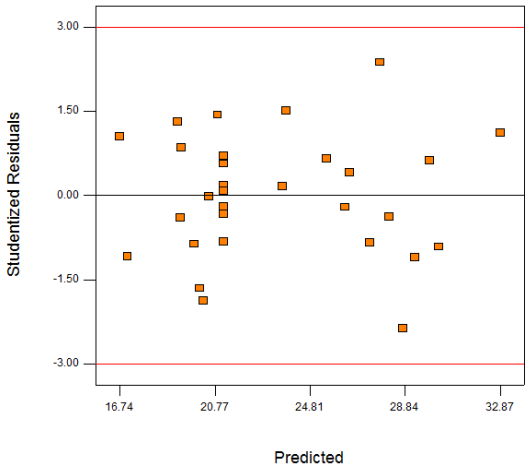

Fig. 4 Predicted oil flotation efficiency and studentized residual plot.

Table 4. Design of experimental runs with coded values and results.

Standard Order	Run order	Coded level of parameters				Observed results Flotation Efficiency (%)	
		Temperature (^{o}C)	pH	Duration (mins)	Flow rate (ml/s)	Actual	Model predicted
1	29	-1	-1	-1	-1	17.18	16.74
2	15	1	-1	-1	-1	20.50	20.51
3	24	-1	1	-1	-1	21.23	21.16
4	19	1	1	-1	-1	24.43	23.79
5	21	-1	-1	1	-1	16.61	17.07
6	11	1	-1	1	-1	19.73	19.18
7	25	-1	1	1	-1	28.76	27.76
8	4	1	1	1	-1	27.76	28.75
9	23	-1	-1	-1	1	21.49	20.89
10	27	1	-1	-1	1	26.19	26.28
11	17	-1	1	-1	1	19.72	19.36
12	6	1	1	-1	1	23.69	23.62
13	26	-1	-1	1	1	25.78	25.51
14	13	1	-1	1	1	28.78	29.24
15	18	-1	1	1	1	29.88	30.26
16	7	1	1	1	1	33.34	32.87
17	28	-2	0	0	0	19.43	20.12
18	1	2	0	0	0	26.67	26.50
19	16	0	-2	0	0	19.13	19.30
20	30	0	2	0	0	26.99	27.34
21	22	0	0	-2	0	19.51	20.29
22	9	0	0	2	0	30.13	29.87
23	2	0	0	0	-2	19.54	19.90
24	14	0	0	0	2	28.01	28.17
25	20	0	0	0	0	21.46	21.13
26	3	0	0	0	0	21.54	21.13
27	10	0	0	0	0	20.64	21.13
28	8	0	0	0	0	20.93	21.13
29	12	0	0	0	0	21.17	21.13
30	5	0	0	0	0	21.01	21.13

Table 5. Analysis of variance (ANOVA) of the response surface model to predict flotation efficiency.

Source/ Operating parameters	Sum of squares	Degree of freedom	Mean square	F value	Prob > F
Model (Y)	540.08	14	38.58	91.59	< 0.0001
A (X_1)	60.96	1	60.96	144.73	< 0.0001
B (X_2)	97.08	1	97.08	230.48	< 0.0001
C (X_3)	137.52	1	137.52	326.49	< 0.0001
D (X_4)	102.55	1	102.55	243.46	< 0.0001
A^2	8.19	1	8.19	19.44	0.0005
B^2	8.26	1	8.26	19.62	0.0005
C^2	26.82	1	26.82	63.67	< 0.0001
D^2	14.52	1	14.52	34.47	< 0.0001
AB	1.27	1	1.27	3.02	0.1028
AC	2.73	1	2.73	6.48	0.0224
AD	2.63	1	2.63	6.25	0.0245
BC	39.47	1	39.47	93.70	< 0.0001
BD	35.31	1	35.31	83.84	< 0.0001
CD	18.43	1	18.43	43.74	< 0.0001
Residual	6.32	15	0.42		
Lack of Fit	5.75	10	0.57	5.01	0.0446
Pure Error	0.57	5	0.11		

The coefficient of determination was evaluated together with the ANOVA statistical analysis to estimate the quality of the model as shown in Table 5. The probability values (P-values) presented in Table 5 showed that all independent parameters were significant (P-values < 0.05) for determining the flotation efficiency. The coefficients of multiple determinations R^2 and R^2_{adj} was found to be and 0.9379 and 0.9776 respectively. The high value of R^2 shows that the model-predicted values co-relates well with the experimental values. This was in good agreement with the actual and predicted flotation efficiency plot as shown in Fig. 5. The good correlation coefficients implied that the quadratic model is a good representation of the experimental system.

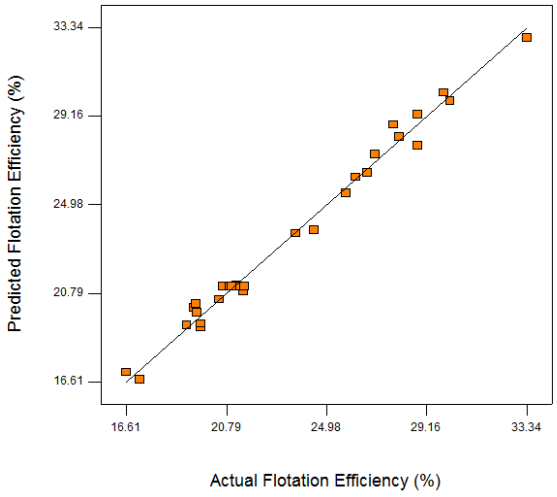

Fig. 5. Actual and predicted plot of oil flotation efficiency (%).

3.4. Perturbation plot

The perturbation plot (Fig. 6) was analysed in order to identify the sensitive parameters that significantly affect the flotation process. According to the perturbation plot, all four parameters (temperature, pH, experimental duration and input flow rate) appeared to be influential in increasing the flotation efficiency.

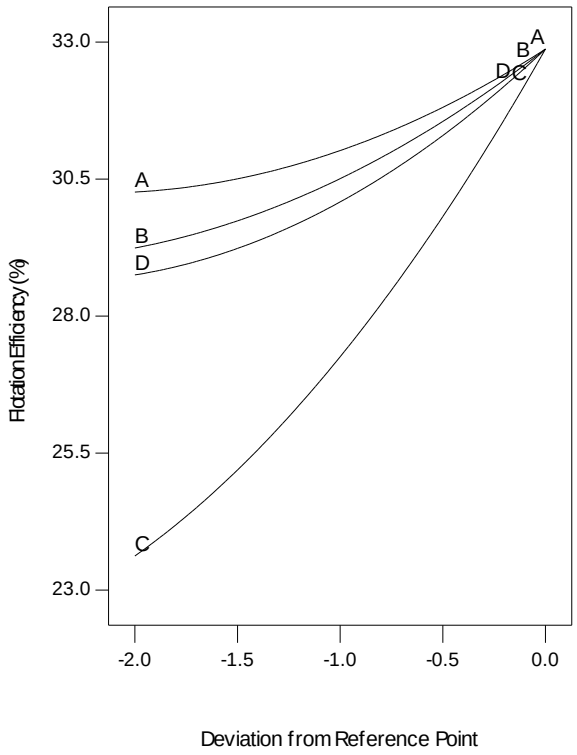

Fig. 6. Perturbation plot for flotation efficiency (%) [Note: A = temperature (X_1), B = pH (X_2), C = duration of flotation (X_3), D = input flow rate (X_4)].

Figure 6 indicated that the increase in the temperature resulted in a slightly enhanced bunker oil removal, as it does not appear to be as significant as the other parameters. This is probably attributed to the lack of change in the bubble diameter with the increase in temperature as shown earlier in Table 2, which implies that the specific surface area and air bubble flux is constant. Hence, the probability of air bubbles attached to the oil is constant with respect to the change in temperature, which leads to a less significant oil removal efficiency. Nevertheless, the increase in temperature is important to decrease the oil density and viscosity, which could lead to the increase in flotation efficiency.

The pH also influenced the flotation efficiency where the oil removal increased with increasing pH. This is attributed to the increase in repulsive forces between oil and sand [25]. At lower pH, a low removal of oil from contaminated sand was recorded due to the weak repulsive forces and highly attractive forces between oil and sand. Further increase in pH due to the addition of NaOH contributes to the release of natural surfactants (carboxylate salt) from the saponification reaction which weakens the interaction attractive forces between

oil and sand. This subsequently leads to a significant increase in the flotation efficiency [26]. In addition, the increase in pH also decreases the Sauter mean diameter of bubbles produced due to the decrease in bubble coalescence. A smaller bubble diameter leads to a greater air bubble specific surface area and air bubble flux, which then causes the increase in oil flotation efficiency as observed.

The input flow rate parameter and experimental duration also influenced the flotation efficiency since the controlled flow rate determines the air bubble parameters. For a constant time frame, an increase in the flow rate decreases the bubble diameter and increases air bubble surface area as well as air bubble flux in a flotation cell as seen earlier in Table 2. A small bubble diameter with a large surface area and bubble flux is advantageous for flotation application, as it increases the attachment probability of bubble to the oil contaminant. This would therefore aid the flotation of oil contaminant to the oil contaminant. Likewise for a constant input flow rate, the increase in experimental duration also increases the bubble concentration within the flotation cell. Therefore, the increase in bubble count increases the chances for bubble-oil attachment and increases the probability of collision, which in turn helps to remove oil from sand. Hence, this leads to an increase in the oil removal efficiency, as evident in Fig. 6.

3.5. Interaction effects of parameters

In order to gain a better understanding of the interaction effects between the input parameters, three-dimensional (3-D) plots for the measured response were drawn based on the model equations from the Design Expert Software. Figures 7(a) –(f) shows the 3D surface response and counter plots on the interaction effects of two input parameters. The remaining parameters were held constant, and were chosen based on the maximum output (flotation efficiency).

Figure 7(a) shows the 3D response surface relationship between temperature (X_1) and pH (X_2) on the flotation efficiency, keeping experimental duration (X_3) and flow rate (X_4) constant. Here, it can be observed that the flotation efficiency is affected by the change in both temperature and pH. An increase in flotation efficiencies could be significantly achieved with the increase in both the temperature and pH. Figure 7(b), which shows the relationship between temperature (X_1) and duration of flotation experiment (X_3), shows an increase in flotation efficiency with the increase in temperature and experimental duration. The effect of experimental duration (X_3) is more pronounced and could be seen to highly influence the flotation efficiency by 10% with the increase in experimental duration from 10 to 20 minutes. The effect of temperature (Fig. 7(a)) was less significant compared to the effect of experimental duration in Fig. 7(b). Figure 7(c), which depicts the response surface relationship between temperature (X_1) and input flow rate (X_4) shows similar pattern with Fig. 7(a), indicating that the increase in both temperature and input flow rate increases the flotation efficiency.

In contrast, Fig. 7(d) which shows the relationship between pH (X_2) and duration (X_3) on flotation efficiencies (%) displayed similar behaviour with Fig. 7(b) as well whereby the effect of experimental duration is much more significant compared to the effect of pH. Likewise, the increase in both pH and experimental duration increased the flotation efficiency. In Fig. 7(e), the response surface plots shows the effect of pH (X_2) and input flow rates (X_4) on flotation efficiencies (%).

Here, both pH and input flow rate parameters were observed to play a significant role in the flotation efficiency, with the increase in both pH and input flow rate to maximum showed highest flotation efficiency recorded. Lastly, Fig. 7(f) which shows the 3-D response surface relationship between duration (X_3) and input flow rates (X_4), shows that the maximum flotation efficiency could be observed with the increase in experimental duration and input flow rate. As observed, experimental duration showed a domineering trend over input flow rates on the flotation efficiency output.

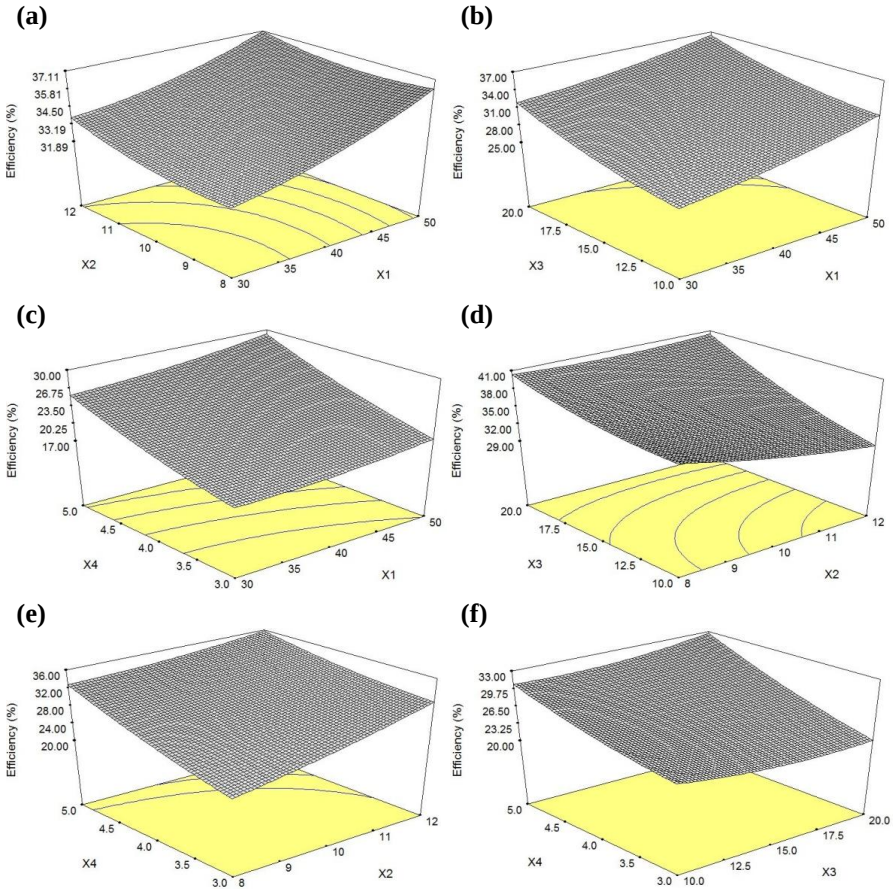

Fig. 7. Response surface plots of flotation efficiencies (%) due to: (a) effect of temperature (X_1) and pH (X_2); (b) effect of temperature (X_1) and duration (X_3); (c) effect of temperature (X_1) and input flow rates (X_4); (d) effect of pH (X_2) and duration (X_3); (e) effect of pH (X_2) and input flow rates (X_4); (f) effect of duration (X_3) and input flow rates (X_4).

3.6. Control and optimization studies

Based on the model, the optimum flotation parameters were found to be at temperature of 60 ^{o}C, pH 8, flotation duration of 20 minutes, and a water input flow rate of 6L/min, with a prediction of 40.4% in flotation efficiency. The values were experimentally validated via flotation experiments with the corresponding flotation

efficiency of 40.1 % (S.D. 1.98), which is in good agreement with the predicted value through empirical results. This confirms that RSM could be effectively used to optimize the process parameters using the statistical design of experiments.

A control experiment was also conducted whereby the flotation is attempted without the usage of any bubbles using the optimized flotation parameters found. The purpose of this control study is to observe the effect of natural oil buoyancy for bunker oil separation. The flotation efficiency of bunker oil without the usage of bubbles under the above optimized conditions is 2.88%. It could be concluded that the presence of microbubbles therefore aids the flotation of bunker oil for enhanced flotation efficiency. This could be attributed to air bubble buoyancy which assists the flotation of bunker oil in the flotation system.

Nevertheless, the flotation efficiencies using microbubbles for the removal of bunker oil from oil-wet sand is still insufficient for industrial applications even at optimized conditions. This is attributed to the high interaction forces between the oil and sand particles which makes it difficult for the liberation of oil from contaminated sands [26]. To minimize the effect of attachment forces on the flotation efficiency, the flotation experiment were subsequently conducted using water-wet sands (defined as wet sand contaminated with oil) under the same conditions as shown in Fig. 8. The presence of water could weaken the interaction forces between the oil layer and sand particles, easing the removal of oil from contaminated soil. At the above mentioned optimum flotation parameters, the increase in water content from 0 to 8 wt% increased the removal of oil from sand by approximately 35%. Therefore, the removal of oil in water-wet sands is more efficient than oil-wet sands as the oil contaminant is not directly in contact with the sand which weakens the attachment forces between sand and oil, leading to higher flotation efficiency.

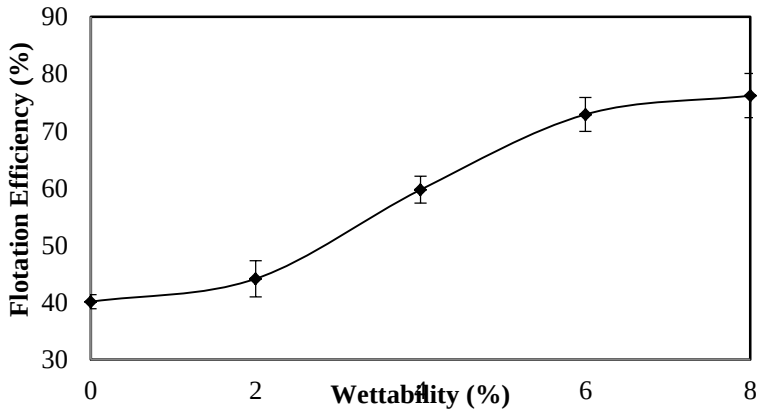

Fig. 8. Effect of wettability on the flotation efficiency of oil-contaminated sands at 60 ^{o}C, pH 8, 20 minutes, input flow rate of 6 L/min.

4. Conclusions

This paper studies the optimization of flotation technology using microbubbles with average Sauter diameter of 80 μm for oil removal from contaminated sand. The effect of temperature, pH, experimental duration and input flow rate had been investigated for bunker oil flotation in a laboratory-scale flotation cell using an

RSM optimization study. The concluding observations from this study are summarized as below.

- The optimized flotation parameters of pH 8, 20 minutes, 60 ^{o}C and 6 L/min input flow rate yields flotation efficiencies of 40.1% under oil-wet condition.
- Further investigations demonstrated that the flotation efficiency at optimized conditions increased from 40.1% to 76.2% with increase in water content in sand from 0 to 8 wt%.
- The influence of bubble is evident, as the presence of bubbles significantly enhanced the flotation efficiency from 3% to 40% in oil-wet sand. This was attributed to the buoyancy of the bubbles which aid the flotation of bunker oil.
- While the presence of microbubbles increased the flotation efficiencies, as compared to a natural bunker oil flotation, the efficiencies recorded is still insufficient for industrial purposes, mainly attributed to the properties of oil-wet sands. Future work is required to further improve the flotation efficiency results for the bunker oil contamination on beach sand, by reducing the attachment forces between oil and sand particles.

Acknowledgements

The authors gratefully acknowledge the Ministry of Higher Education (MOHE) Malaysia for the Fundamental Research Grant Scheme (FRGS, Grant No.: FRGS/1/2015/TK07/MUSM/03/2), Monash University Malaysia for providing research facilities.

References

1. Tao, D. (2005). Role of bubble size in flotation of coarse and fine particles - A review. *Separation Science and Technology*, 39(4), 741-760.
2. Zhou, Z.; Chow, R.; Cleyle, P.; Xu, Z.; and Masliyah, J. (2010). Effect of dynamic bubble nucleation on bitumen flotation. *Canadian Metallurgical Quarterly*, 49(4), 363-372.
3. Andy Hong, P.K.; Cha, Z.; Zhao, X.; Cheng, C.-J.; and Duyvesteyn, W. (2013). Extraction of bitumen from oil sands with hot water and pressure cycles. *Fuel Processing Technology*, 106, 460-467.
4. Al-Otoom, A.; Allawzi, M.; Al-Harahsheh, A.M.; Al-Harahsheh, M.; Al-Ghbari, R.; Al-Ghazo, R.; and Al-Saifi, H. (2009). A parametric study on the factors affecting the froth floatation of Jordanian tar sand utilizing a fluidized bed floatator. *Energy*, 34(9), 1310-1314.
5. Wang, J.; Yin, J.; Ge, L.; and Zheng, J. (2009). Using flotation to separate oil spill contaminated beach sands. *Journal of Environmental Engineering*, 136(1), 147-151.
6. Long, J.; Drelich, J.; Xu, Z.; and Masliyah, J.H. (2007). Effect of operating temperature on water‐based oil sands processing. *The Canadian Journal of Chemical Engineering*, 85(5), 726-738.

7. Kim, T.-I.; Kim, Y.-H.; Han, M. (2012). Development of novel oil washing process using bubble potential energy. *Marine Pollution Bulletin*, 64(11), 2325 - 2332.
8. Wills, B.A. and Napier-Munn, T. (2006). *Wills's mineral processing technology: an introduction to the practical aspects of ore treatment and mineral recovery* (7th ed.). USA: Butterworth-Heinemann.
9. Urum, K.; Grigson, S.; Pekdemir, T.; and McMenamy, S. (2006). A comparison of the efficiency of different surfactants for removal of crude oil from contaminated soils. *Chemosphere*, 62(9), 1403-1410.
10. Zhang, L.; Somasundaran, P.; Ososkov, V.; and Chou, C. (2000). Flotation of hydrophobic contaminants from soil. *Colloids and Surfaces A: Physicochemical and Engineering Aspects*, 177(2), 235-246.
11. Chou, C.-C.; Ososkov, V.; Zhang, L.; and Somasundaran, P. (1998). Removal of nonvolatile hydrophobic compounds from artificially and naturally contaminated soils by column flotation. *Journal of Soil Contamination*, 7(5), 559-571.
12. Masliyah, J.; Zhou, Z.J.; Xu, Z.; Czarnecki, J.; and Hamza, H. (2004). Understanding water‐based bitumen extraction from athabasca oil sands. *The Canadian Journal of Chemical Engineering*, 82(4), 628-654.
13. Urum, K.; Pekdemir, T.; and Çopur, M. (2004). Surfactants treatment of crude oil contaminated soils. *Journal of Colloid and Interface Science*, 276(2), 456-464.
14. Czarnecki, J.; Radoev, B.; Schramm, L.L.; and Slavchev, R. (2005). On the nature of Athabasca Oil Sands. *Advances in Colloid and Interface Science*, 114–115, 53-60.
15. Hupka, J.; Miller, J.D.; and Drelich, J. (2004). Water-based bitumen recovery from diluent-conditioned oil sands. *The Canadian Journal of Chemical Engineering*, 82(5), 978-985.
16. Painter, P.; Williams, P.; and Lupinsky, A. (2010). Recovery of bitumen from Utah tar sands using ionic liquids. *Energy & Fuels*, 24(9), 5081-5088.
17. Tsai, J.-C.; Kumar, M.; Chen, S.-Y.; and Lin, J.-G. (2007). Nano-bubble flotation technology with coagulation process for the cost-effective treatment of chemical mechanical polishing wastewater. *Separation and Purification Technology*, 58(1), 61-67.
18. Aslan, N.; and Fidan, R. (2008). Optimization of Pb flotation using statistical technique and quadratic programming. *Separation and Purification Technology*, 62(1), 160-165.
19. Wei, T.K.; and Manickam, S. (2012). Response Surface Methodology, an effective strategy in the optimization of the generation of curcumin‐loaded micelles. *Asia‐Pacific Journal of Chemical Engineering*, 7(Issue Supplement S1), 125-133.
20. Kalyani, V.; Pallavika, Gouri Charan, T.; and Chaudhuri, S. (2005). Optimization of a laboratory-scale froth flotation process using response surface methodology. *Coal Preparation*, 25(3), 141-153.

21. Tir, M.; and Moulai-Mostefa, N. (2008). Optimization of oil removal from oily wastewater by electrocoagulation using response surface method. *Journal Of Hazardous Materials*, 158(1), 107-115.
22. Nassif, M.; Finch, J.A.; and Waters, K.E. (2014). Determining frother-like properties of process water in bitumen flotation. *Minerals Engineering*, 56, 121-128.
23. Sishtla, C.; Chan, I.; and Knowlton, T. (1986). The effect of temperature on bubble parameters in fluidized beds. *Fifth International Fluidization Conference*. Elsinore, Denmark.
24. Watcharasing, S.; Kongkowit, W.; and Chavadej, S. (2009). Motor oil removal from water by continuous froth flotation using extended surfactant: effects of air bubble parameters and surfactant concentration. *Separation and Purification Technology*, 70(2), 179-189.
25. Liu, J.; Xu, Z.; and Masliyah, J. (2005). Interaction forces in bitumen extraction from oil sands. *Journal of Colloid and Interface Science*, 287(2), 507-520.
26. Lim, M.W.; Lau, E.V.; Poh, P.E.; and Chong, W.T. (2015). Interaction studies between high-density oil and sand particles in the oil flotation technology. *Journal of Petroleum Science and Engineering*, 131, 114-121.